

Cationic surfactant-assisted foam fractionation enhances the removal of short-chain perfluoroalkyl substances from impacted water



Cheng-Shiuan Lee^a, Arjun K. Venkatesan^{b,*}

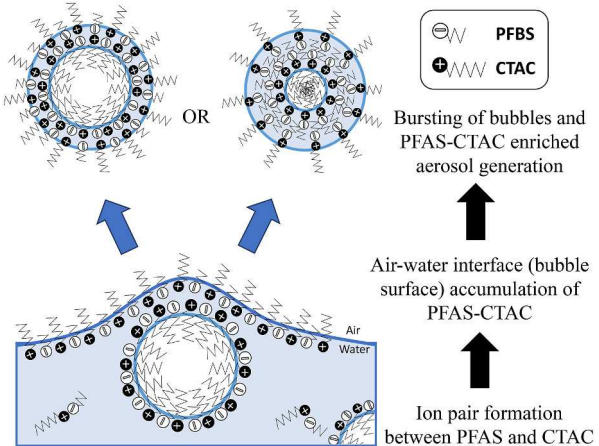
^a Research Center for Environmental Changes, Academia Sinica, Taipei, 115, Taiwan

^b Department of Civil and Environmental Engineering, New Jersey Institute of Technology, Newark, NJ, 07102, USA

HIGHLIGHTS

- Cationic surfactant enhanced short-chain PFAS removal during foam-fractionation.
- Ion-pair formation between PFAS and CTAC increased surface activity of short-chains.
- Aerosolization was the primary pathway for PFAS removal in non-foaming waters.
- Mass balance of PFAS in the system can achieve 70–100% when aerosols were measured.

GRAPHICAL ABSTRACT



ARTICLE INFO

Handling editor: Dr Y Yeomin Yoon

Keywords:

Foam fractionation
Bubbling
Aerosols
Ion pair
CTAC
PFAS

ABSTRACT

Several studies have demonstrated that air-bubbling and foam fractionation techniques can efficiently remove long-chain PFAS from contaminated water. However, removing short-chain PFAS is challenging due to its lower surface activity and inability to form self-assembly structures at the air-water interface. In this study, we tested various additives, including salts, surfactants, and polymers, to improve short-chain PFAS (e.g., perfluorobutanesulfonic acid (PFBS) and perfluorobutanoic acid (PFBA)) removal in non-foaming solutions using a bench-scale system. We found that in the presence of cetyltrimethylammonium chloride (CTAC) and salt, air-bubbling can significantly remove $0.5 \mu\text{g L}^{-1}$ of PFBS and PFBA in deionized water by >99% (15 min) and 81% (60 min), respectively. The decline of surface tension and the formation of thin foam-like layers during bubbling, controlled by the concentration of CTAC, significantly improved the removal of short-chain PFAS. Adding anionic and neutral surfactants showed no removal of short-chain PFAS during bubbling, suggesting the importance of the electrostatic interactions between short-chain PFAS and the cationic CTAC. We observed a 1:1 M ratio between CTAC and PFBS removed from the solution, suggesting the formation of ion pairs in the solution and enhancing the surface activity of the overall neutral (PFAS-CTAC) complex. A mass balance of the system

* Corresponding author.

E-mail address: arjun.venkatesan@njit.edu (A.K. Venkatesan).

revealed that the primary mechanism by which PFAS was removed from non-foaming waters was through aerosol generation (70–100%). Using the optimized condition, PFAS mixtures (short- and long-chain PFAS, including five recently regulated PFAS by USPEA, 2 nM each) in deionized water and natural groundwater were successfully removed to below detection (>99% removal; <2 ng L⁻¹), except for PFBA (25–73% removal). These results provide an improved understanding of the mechanism by which PFAS is removed during foam fractionation and highlight the need for capturing aerosols enriched with PFAS to prevent secondary contamination.

1. Introduction

Per- and polyfluoroalkyl substances (PFAS) are a group of emerging contaminants that contain multiple carbon-fluorine bonds, making them possess unique physical and chemical properties for wide application in commercial and industrial products (Buck et al., 2011; Evich et al., 2022). To date, over 14,000 PFAS are listed in the U.S. EPA's CompTox chemical dashboard (U.S. Environmental Protection Agency, 2023). PFAS detection in products surrounding us has been continuously reported (Muensterman et al., 2022; Thompson et al., 2023; Xia et al., 2022), suggesting their ubiquitousness. PFAS are the primary ingredient of aqueous film-forming foams (AFFF) used to extinguish flammable liquid fires such as fuel fires. Routine fire drills conducted in fire departments, airports, and military facilities are a major source of PFAS contamination entering groundwater and surface water. Contaminated drinking water is considered the primary exposure route to humans (Sunderland et al., 2019), and adverse health effects due to PFAS exposure have been studied and reported extensively (Fenton et al., 2021; Pelch et al., 2019). PFAS are often called 'forever chemicals' because they are highly persistent in the environment and are resistant to conventional water/wastewater treatment processes (Londhe et al., 2021; Venkatesan and Halden, 2013; Venkatesan et al., 2022). As regulations and guidelines for PFAS evolve in many U.S. states and countries worldwide, the need for PFAS removal techniques in water becomes an urgent mission. Thus, advanced water treatment technologies, including separation and destruction approaches, have been developed and/or tested for PFAS removal in the past few decades (Kucharzyk et al., 2017; Nzeribe et al., 2019; Rahman et al., 2014). Destruction technologies for PFAS removal require high energy consumption (Londhe et al., 2021). Separation and sorption treatments are more accessible and cost-efficient. For instance, granular activated carbon (GAC), ion-exchange resin (IX resin), nanofiltration, and foam fractionation have all been investigated for removing PFAS in contaminated waters (Burns et al., 2021; Dixit et al., 2021; Du et al., 2014; Franke et al., 2019). However, concentrated PFAS waste generated after the treatment needs further disposal. Studies have proposed that a treatment train, combining sequestration and destruction technologies, is required to concentrate and destroy PFAS (Lu et al., 2020).

PFAS are surface active and can form self-assembly structures at the air-water interface. Recent works acknowledge the importance of the air-water partitioning of PFAS (Costanza et al., 2019; Schaefer et al., 2019), which could influence the overall performance of treatment systems. For example, PFAS adsorption onto carbonaceous materials has been shown to be enhanced by the presence of air bubbles on carbon surfaces (Meng et al., 2014, 2020). The researchers showed that perfluorooctanesulfonic acid (PFOS) adsorption on several carbonaceous adsorbents decreased by up to 80% after vacuum degassing. Their proposed mechanism involved the preferential adsorption of the oleophobic/hydrophobic tail of PFOS into the air bubble on the adsorbent surface, while the polar sulfonic head group exists in the aqueous solution near the interface. Furthermore, these authors showed that upon removal of air bubbles by centrifugation, up to 80% of PFAS were able to desorb from the sorbent (Meng et al., 2020). Some studies have utilized air bubbling to remove PFAS directly from solutions, an approach called foam fractionation, and successfully demonstrated the capacity of air bubbles as a carrier to move PFAS from the bulk solution (Ebersbach et al., 2016; Wang et al., 2018). Researchers have shown that PFAS,

specifically perfluorooctanoic acid (PFOA) and PFOS, can be efficiently removed (>99%) from the solution and enriched in bursting aerosols under certain conditions. For example, higher ionic strength or salinity favors PFAS removal by bubbling (Buckley et al., 2022; Ebersbach et al., 2016; Morrison et al., 2023), and also the addition of cations (e.g., Fe (III), La(III), Al(III)) serving as a metallic activator enhances removal (Lee et al., 2017). Both high and low solution pH have demonstrated favorable removal of PFAS by bubbling, and this might be associated with the mineral acids used for pH adjustment, in which cations were introduced simultaneously (Meng et al., 2018; Zhang and Liang, 2020). Bubble size and the length of their traveling path (from the bottom to the top) also influence the degree of PFAS removal; smaller bubbles and a longer path can extract more PFAS from the solution (Buckley et al., 2023b; Cao et al., 2019; Ebersbach et al., 2016). The PFAS removal capacity can also be slightly improved in solutions with a lower temperature (Morrison et al., 2023). Applying surfactants or polymer additives to the solution has improved PFAS removal efficiencies for certain compounds (Bolto and Xie, 2019; Buckley et al., 2023a; Li et al., 2021; Vo et al., 2023). Long-chain PFAS (fluorinated C ≥ 6) in landfill leachate was shown to be effectively extracted (80–100%) into the bubbling-induced foam layer for further separation (Burns et al., 2022; McCleaf et al., 2021; Robey et al., 2020; Smith et al., 2022). A few recent studies using pilot and large-scale foam fractionation systems for treating PFAS-contaminated water also showed promising results in removing over 90% of long-chain PFAS (Burns et al., 2021; Smith et al., 2023). Furthermore, Wang et al. (2023) reported the effective removal of both targeted and non-targeted PFAS (especially those with longer chain lengths and surface-active head groups) in landfill leachate, wastewater treatment plant effluent, and AFFF-contaminated groundwater by foam fractionation.

Dissolved air flotation (DAF) is an existing water treatment process that utilizes coagulants and air bubbles to remove suspended coagulated/flocculated contaminants in water. Similar to observations made in foam fractionation studies, research has shown that only long-chain PFAS (e.g., PFOS) were partially removed in DAF systems with alum as the coagulant (Thompson et al., 2011). Other types of coagulants, like polyelectrolytes (PES) with positive charges and hydrophobic structures, may enhance PFAS removal in DAF systems (Bolto and Xie, 2019). Although many studies have been done with respect to bubbling-assisted PFAS removal in solutions, contradictory results often exist, which could likely be attributed to the differences in water matrices tested and in the design of aeration devices among studies. For example, Buckley et al. (2023a) reported ~100% removal of perfluorobutanoic acid (PFBA) in pure water within 60 min by air bubbling with cetyltrimethylammonium chloride (CTAC) addition, while the same device with similar conditions used in another study (Vo et al., 2023) failed to remove PFBA (~0%) in landfill leachate. In another example, long-chain PFOS and PFOA were removed poorly (<10%) by bubbling without adding any additives (Lee et al., 2017; Li et al., 2021); whereas some studies showed long-chain PFAS can be efficiently removed (70–100%) by foam fractionation (Ebersbach et al., 2016; Nguyen et al., 2024; Wang et al., 2023). Another critical challenge, in addition to contradictory reports, observed in foam fractionation systems is the poor removal of short-chain PFAS, which has been associated with the low surface activity of short-chain PFAS compared to long-chain PFAS. Also, as most previous applications were focused on the removal efficiency of PFAS, a detailed assessment of PFAS mass balance in the treatment

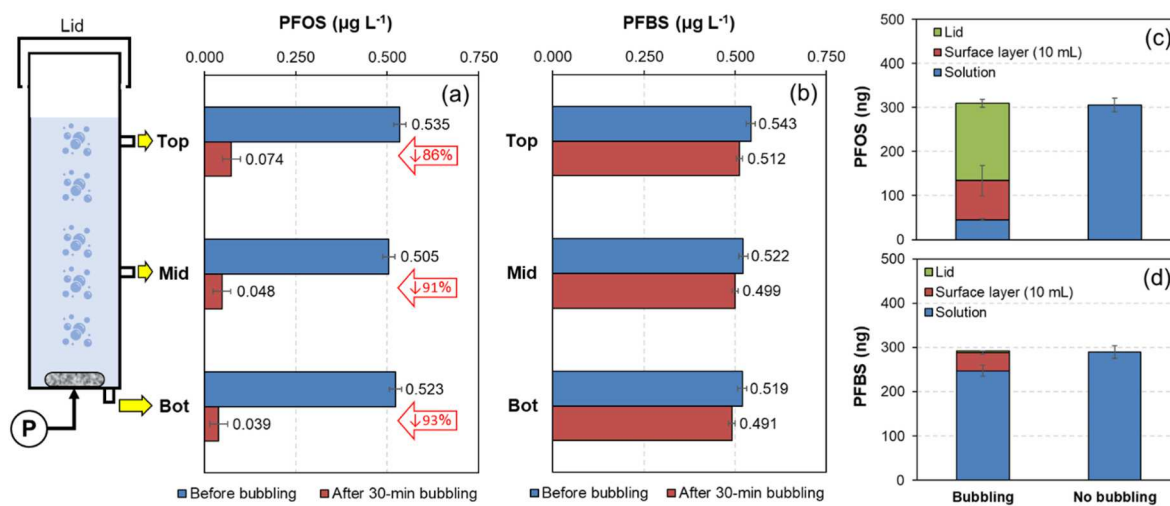


Fig. 1. Concentrations of (a) PFOS and (b) PFBS in the solution collected from three different layers of the water column before and after bubbling. PFAS mass balance of (c) PFOS and (d) PFBS before and after bubbling. Error bars represent the standard deviation of the analytical replicates.

system was often omitted (i.e., lack of reporting on the compartmentalization of PFAS in aerosol and foam fractions). The primary goal of this study was to perform a comprehensive assessment to address the above-mentioned knowledge gaps with regard to the foam fractionation process, with a focus on non-foaming waters. The specific objectives of the present study were to (i) explore the use of air bubbles to effectively extract and remove short-chain PFAS from non-foaming waters (e.g., drinking water, groundwater); (ii) perform a mass balance on a bench-scale foam fractionation system to assess the compartmentalization of PFAS after treatment (i.e., in aerosols and foam fractions); (iii) assess the impact of salts, cationic polymers, and co-surfactants on the removal of short-chain PFAS during foam fractionation of non-foaming waters, and (iv) elucidate the mechanism by which PFAS is removed in non-foaming waters during bubbling treatment.

2. Materials and methods

2.1. Chemicals

Neat materials (purity >97%) of individual PFAS, such as PFBA, PFBS (perfluorobutanesulfonic acid), PFHxA (perfluorohexanoic acid), HFPO-DA (hexafluoropropylene oxide dimer acid), PFHxS (perfluorohexanesulfonic acid), PFOA, PFOS, and PFNA (perfluorononanoic acid), were purchased from Sigma-Aldrich (St. Louis, MO). Isotopically labeled PFAS standards were acquired from Wellington Laboratory (Ontario, Canada). Salts (i.e., NaCl, CaCl₂, Na₂SO₄), polymer (Poly-DADMAC (PDM)), and surfactants (cetyltrimethylammonium chloride (CTAC), dodecytrimethylammonium chloride (DTAC), sodium dodecyl sulfate (SDS), and Brij® L4 were purchased from Sigma-Aldrich (St. Louis, MO). LC-MS grade organic solvents such as methanol, acetonitrile, and isopropanol, and ultrapure Milli-Q® water (MQW, 18.2 MΩ cm) were used throughout this study.

2.2. Bubbling device setup and experimental design

A cylindrical HDPE container (diameter: 50 mm, height: 360 mm, total volume: up to 700 mL) served as the water reservoir. An air bubble diffuser was placed at the bottom of the cylinder and attached to a compressed air tank. A lid was placed on top of the cylinder to collect aerosols. Three water sampling ports were located at the bottom, middle, and upper part (~2 cm below the air-water interface) of the cylinder (Fig. 1).

Firstly, we used PFOS (long-chain) and PFBS (short-chain) as model

PFAS compounds to perform a mass balance in our device. The water volume used in each experiment was 500 mL and the initial PFAS concentration was 0.5 $\mu\text{g L}^{-1}$. The bubbling rate was fixed at 0.5 L min^{-1} and the bubbling time was set at 30 min for preliminary testing. After bubbling, multiple fractions that could contain PFAS were collected, including solutions sampled from the three ports (sampled by 2 mL syringe), 10 mL water from the top surface layer (by pipetting water out with care near the air-water interface), aerosols collapsed on the lid (rinsed by methanol), sorption onto the cylinder wall (rinsed by methanol after emptying the cylinder). Second, different additives (e.g., salts, polymer, surfactants) were added to test the bubbling performance with the same experimental setup described above, but the concentration of salts and additives was varied to evaluate the optimal condition. Before and after bubbling, water samples were collected at the bottom and middle of the cylinder to confirm the remaining PFAS in bulk solution. PFAS attached to the lid were also collected after bubbling to account for aerosolized PFAS. Lastly, the influence of PFAS mixture (equimolar mixture: PFBA + PFBS + PFHxA + HFPO-DA + PFHxS + PFOA + PFOS + PFNA, 2 nM each) and different water matrix (pure water and contaminated Long Island groundwater) was tested with the selected optimized condition.

Time course experiments were conducted to examine the kinetics of PFAS removal in the presence of additives/modifiers. Samples were collected at $t = 5, 15$, and 30 min. The collection time was up to 120 min, if necessary, depending on the chain length of the tested PFAS. Water samples were collected at the bottom and middle of the cylinder at each time point, and after bubbling, PFAS on the lid was recovered by rinsing with methanol.

2.3. Analytical methods

Collected water and methanol-rinsed samples were diluted to 1:1 methanol:water and fortified with isotopically labeled PFAS as internal standards. PFAS was analyzed by a liquid chromatography-tandem mass spectrometer (LC-MS/MS, Agilent 6495B) with negative electrospray ionization (ESI). The chromatographic separation was performed on a C18 analytical column (Agilent Zorbax Eclipse Plus, 50 \times 3 mm, 1.8 μm) with an Agilent 1290 high-pressure liquid chromatography system. A delay column (Agilent Zorbax Eclipse Plus, 50 \times 4.6 mm, 3.5 μm) was installed between the pump and the multi-sampler to minimize background contamination from solvent, tubing, and pump parts. The solvent degasser was bypassed. Data was acquired by Multiple Reaction Monitoring (MRM) method. Detailed MRM information for PFAS

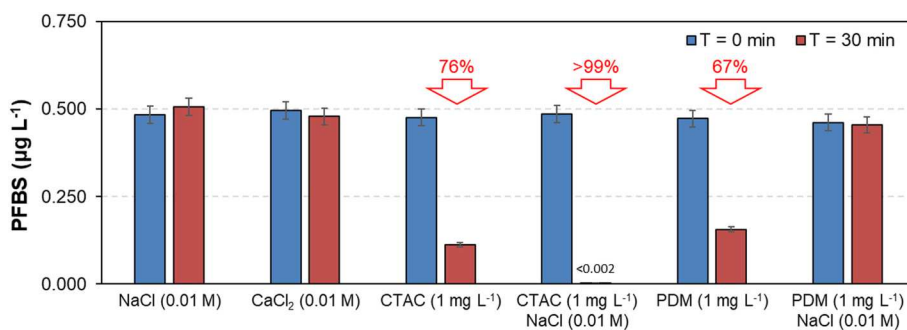


Fig. 2. PFBS concentration in the solution before (blue) and after (red) 30-min of bubbling. Various additives were added to assist bubbling/foam fractionation. The value is the average of the two samples taken from the bottom and middle ports, and the error bar represents the standard deviation. (For interpretation of the references to colour in this figure legend, the reader is referred to the Web version of this article.)

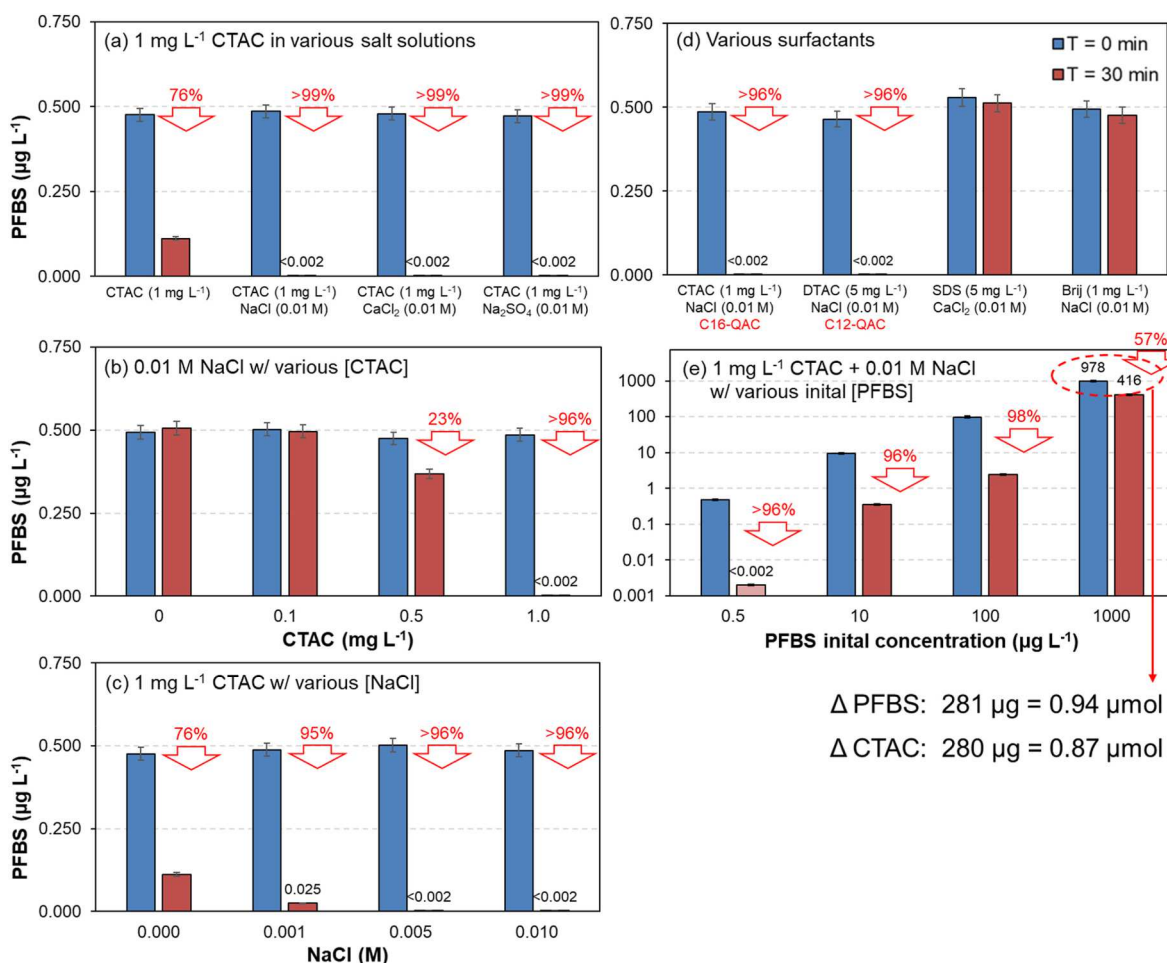


Fig. 3. Optimization of PFBS removal via air bubbling: (a) different types of salts added; (b) varying CTAC concentrations; (c) varying NaCl concentrations; (d) different types of surfactants added; (e) varying PFBS initial concentrations. The error bar represents the standard deviation.

analyzed is listed in Table S1. LC and MS conditions are summarized in Table S2. CTAC analysis was done using the same instrument but with positive ESI. The MRM and instrument conditions for CTAC analysis are shown in Tables S1–S2. Recoveries of eight internal standards were, on average, between 91 and 98% with a standard deviation < 20% (Table S3). The lowest calibration point of all PFAS analyzed was 1 ng L⁻¹ and we conservatively assigned 2 ng L⁻¹ (dilution factor for each sample = 2) as our method detection limit (MDL). The MDL for CTAC was 10 μg L⁻¹ (dilution factor for CTAC samples = 100). Sampling or analytical duplicates were performed to account for experimental/

analytical errors. The relative percent difference (RPD) for each measurement was <10% throughout this study.

Surface tension (ST) was measured by a Sigma 700 force tensiometer (Biolin Scientific, Gothenburg, Sweden) using Du Noüy Ring method. MQW was used as a reference to calibrate the tensiometer (72 mN m⁻¹ at 25 °C). About 100 mL of sample solution was placed in a glass beaker for ST measurement and ten measurements were taken for each sample.

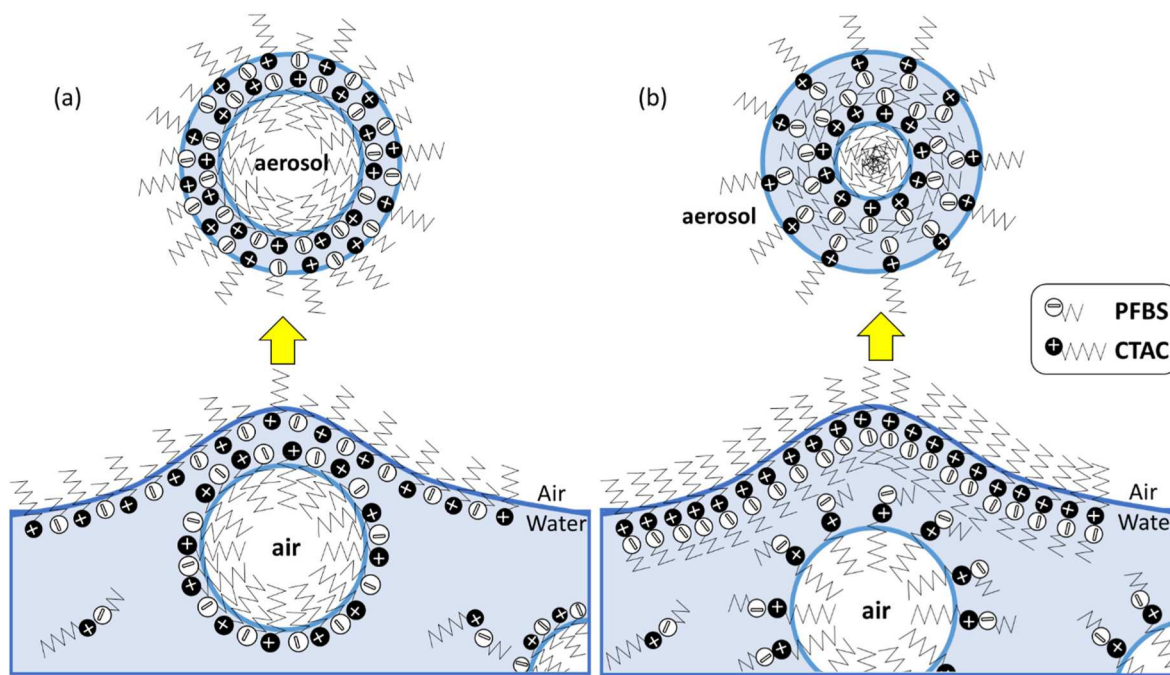


Fig. 4. Proposed interactions between PFBS and CTAC during air bubbling and the formation of aerosols enriched with PFAS-CTAC: (a) PFBS molecule sandwiched between two CTAC molecules at the bubble surface; and (b) CTAC alone occupy the air-water interface at the bubble surface with PFBS electrostatically paired with CTAC head group.

3. Results and discussion

3.1. PFAS mass balance

PFOS (long-chain) and PFBS (short-chain) were used to evaluate the removal of non-foaming water (MQW) and to perform a mass balance in our bubbling device. After 30 min of bubbling, PFOS ($0.5 \mu\text{g L}^{-1}$) in the solution dropped significantly by 86%–93% (Fig. 1a). In contrast, PFBS showed less than 5% decline in the solution (Fig. 1b). The measurements between the samples collected from the top, middle, and bottom ports were similar before bubbling. After bubbling, a slightly increasing trend from the bottom to the top was observed, reflecting PFAS carried by bubbles toward the surface and, therefore, resulting in a heterogeneous distribution of PFAS across the depth of the solution. The mass balance of PFAS in the three fractions can achieve nearly 100% (Fig. 1c and d). After bubbling, ~57% of PFOS was found on the lid, representing the aerosol fraction. Over 29% of PFOS was recovered from the top surface layer (top 10 mL from the surface), and only less than 15% of PFOS remained in the bulk solution (Fig. 1c). Most PFBS remained in the bulk solution (~85%), relatively small amounts of PFBS migrated to the surface (~14%), and nearly no PFBS was found on the lid (<1%).

This result agreed with previous studies as long-chain PFAS (PFOS) feature higher surface activity than short-chains and hence accumulate at the air-water interface (bubble surfaces) more efficiently and are further removed from the solution when continuous bubbles are provided. An important finding in the present study was that the mass balance pointed out aerosolization as the primary mechanism by which PFOS was removed from non-foaming waters (~57%). The lack of stable foams formed in non-foaming waters allows the bubbles to burst and generate PFAS-enriched aerosols that will escape the treatment system if not designed to be captured. Minor enrichment (~8x enrichment) of PFBS at the top surface layer was still observed, but PFBS could not escape from the solution via bursting bubbles and aerosols. Thus, in the following experiments, we focused only on removing short-chain PFAS (e.g., PFBS or PFBA).

3.2. Influence of salts, cationic polymer, and co-surfactants on PFBS removal

PFBS was selected to design a series of experiments to explore the optimal conditions needed to remove short-chain PFAS from contaminated non-foaming waters. Different additives were added to PFBS solutions ($0.5 \mu\text{g L}^{-1}$ in MQW) and the bubbling results are shown in Fig. 2. The addition of salts, Na^+ or Ca^{2+} cations (0.01 M), did not enhance the removal of PFBS in our system. Adding CTAC or PDM (1 mg L^{-1}) greatly improved the removal efficiency by 76% and 67%, respectively. Moreover, adding 1 mg CTAC L^{-1} in the presence of 0.01 M NaCl further removed all PFBS to below the instrumental detection (>99% removal; $<2 \text{ ng L}^{-1}$). Interestingly, the presence of NaCl along with PDM completely diminished the PFBS removal to 0%.

PFBS is not a strong surfactant due to its short fluorinated-alkyl chain length. Surface tension (ST) measurements were used to assess the change in the surface activity of PFBS with the addition of various additives. The ST of $0.5 \mu\text{g PFBS L}^{-1}$ is nearly identical to MQW ($\sim 72 \text{ mN m}^{-1}$) and adding cations (0.01 M Na^+ and Ca^{2+}) did not essentially impact the surface activity of PFBS (70 – 71 mN m^{-1}). Adding CTAC (1 mg L^{-1}) to $0.5 \mu\text{g PFBS L}^{-1}$ lowered the ST to 66.5 mN m^{-1} . We also observed a visible thin foam layer on the surface of the water column during bubbling experiments. We suspect the formation of ion pairs between PFBS and CTAC to be dominant, which has been observed in other co-surfactant systems measured by X-ray reflectivity (Yefet et al., 2014). Hence, PFBS was presumably attracted by CTAC via electrostatic (primary) and hydrophobic (secondary) interactions and then enriched at the air-water interface provided by air bubbling. Aerosols produced by bubble bursting then brought PFBS along with CTAC away from the water column. The ST further decreased in the presence of Na^+ and CTAC (ST: 62.9 mN m^{-1}), resulting in a thicker surface foam layer on the surface of the water column and causing more PFBS-CTAC complex to be removed.

Adding 1 mg L^{-1} PDM did not change the surface tension greatly (ST = $\sim 72 \text{ mN m}^{-1}$). Thus, the observed PFBS removal with PDM might not be related to aerosol formation. PDM is a high molecular weight polymer (colloid) with a positive charge that would electrostatically attract PFBS.

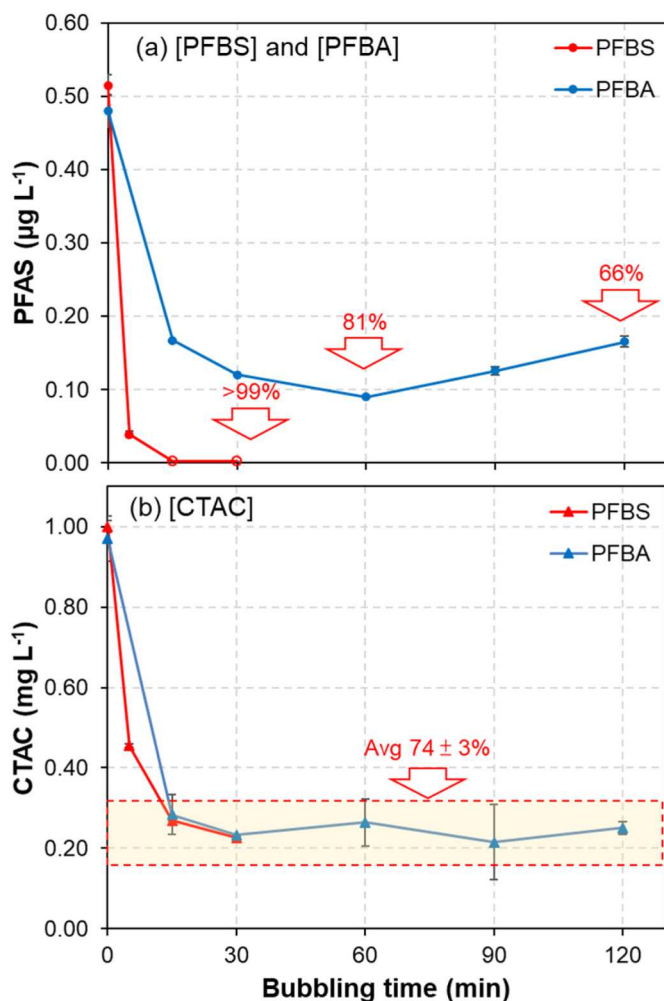


Fig. 5. Time course experiment of bubbling removal for (a) PFBA and PFBS, and (b) CTAC. The error bar represents the standard deviation.

Bubbling can move these PFBS-PDM colloids upward like in DAF systems, and therefore, decreased PFBS was observed in the sample collected from the middle and bottom ports. We confirmed the size fractionation in the PFBS-PDM solution using an Amicon 3 kDa centrifugal ultrafiltration unit and we found that nearly half of the PFBS was associated with PDM (>3 kDa fraction) (Fig. S1a). With bubbling, the dissolved PFBS (<3 kDa) did not change much, but the PFBS-PDM fraction (>3 kDa) declined significantly. Moreover, adding excess chloride (0.01 M NaCl) can inhibit PFBS-PDM interactions, and nearly 100% of PFBS remained in the <3 kDa fraction (Fig. S1b). This result helps confirm our hypothesis that the formation of PFBS-PDM colloids could result in the heterogeneous distribution of PFBS in the solution. Also, this explains that no PFBS decline was observed in the PDM (1 mg L^{-1})-NaCl (0.01 M) solution after bubbling (Fig. 2).

3.3. Optimization of bubbling treatment for non-foaming waters

Different types and concentrations of salts, CTAC, and PFBS were investigated to identify optimal conditions to remove short-chain PFAS. We additionally tested various surfactants with different charges to explore the possible removal mechanism (Fig. 3). Three different salts, NaCl, CaCl₂, and Na₂SO₄ (0.01 M), were tested with 1 mg L⁻¹ CTAC and all of them showed enhanced PFBS removal to below detection ($<2 \text{ ng L}^{-1}$) after bubbling (Fig. 3a). At the same concentration of 0.01 M, Na₂SO₄ has a larger ionic strength and also decreased the surface tension more than the other salts (ST: NaCl = 62.9 mM m⁻¹, CaCl₂ = 61.8 mM

m⁻¹, Na₂SO₄ = 60.0 mM m⁻¹). This may imply that Na₂SO₄ could be a better salt additive for bubbling applications. The initial concentration of CTAC (NaCl fixed at 0.01 M) also strongly influenced the PFBS removal efficiency (Fig. 3b). PFBS was removed by only 23% with 0.5 mg L⁻¹ CTAC and no removal was found when the initial CTAC concentration dropped to 0.1 mg L⁻¹. This could be attributed to the relatively high ST of 0.1 mg L⁻¹ (ST: 70 mM m⁻¹) and 0.5 mg L⁻¹ (ST: 66.6 mM m⁻¹) CTAC solutions, leading to thinner foam layer generation and lesser aerosol formation. As low as 0.001 M NaCl (CTAC fixed at 1 mg L⁻¹) can improve PFBS removal from 76% to 95% in the presence of CTAC (Fig. 3c). Adding more salts could further enhance removal to below detection, as the ST reduces with increasing ionic strength.

To evaluate the importance of the charge group of surfactants, SDS (anionic surfactant) and Brij® L4 (nonionic surfactant) were tested for PFAS removal during foam fractionation. In addition to CTAC (C-16 QAC, quaternary ammonium compound), we included DTAC (C-12 QAC) because it possesses the same hydrophobic alkyl chain length of 12 carbons as SDS and Brij® L4. The results are shown in Fig. 3d and the reason for the different salts and initial concentrations of surfactants used was to maintain a comparable ST among experimental groups. DTAC behaved as good as CTAC, removing >99% of PFBS in the solution. In contrast, the solution with SDS or Brij® L4 showed no PFBS removal after bubbling, suggesting the key role of the charge, especially for short-chain PFAS. In contrast, some studies demonstrated that adding anionic, zwitterionic, or nonionic surfactants to increase foam layer formation can also enhance the bubbling removal of long-chain PFAS to a certain extent (Buckley et al., 2023a; Li et al., 2021). This suggests that as long as more air-water interfaces (e.g., foam layer) can be produced, the strong surface activity of long-chain PFAS allows the molecules to accumulate in the interface and overcome electrostatic repulsion between PFAS and the anionic co-surfactant.

Lastly, we increased the initial concentration of PFBS (10–1000 $\mu\text{g L}^{-1}$) and fixed CTAC (1 mg L⁻¹ CTAC) and NaCl (0.01 M). The removal percentage in a 100 $\mu\text{g L}^{-1}$ PFBS solution can still reach 98% (Fig. 3e). The removal percentage declined to 57% at an initial PFBS concentration of 1000 $\mu\text{g L}^{-1}$, implying insufficient CTAC to interact with PFBS for complete removal. By calculating the amount of PFBS ($\Delta\text{PFBS} = 0.94 \mu\text{mol}$) and CTAC ($\Delta\text{CTAC} = 0.87 \mu\text{mol}$) removed from the solution, we found that the molar ratio between these two compounds was close to 1:1 ($\Delta\text{PFBS}:\Delta\text{CTAC}$). This result gives us a clue about the formation of PFBS-CTAC ion pairs at the air-water interface. Similar to mechanisms suggested in the earlier studies on how cationic surfactants react with PFAS during bubbling (Buckley et al., 2023a; Li et al., 2021), we propose plausible removal mechanisms (Fig. 4). Short-chain PFBS could form ion pairs with CTAC in the solution via electrostatic attraction. At the air-water interface, PFBS-CTAC ion pairs are enriched in bubbles and foams, where two CTAC molecules sandwich one PFBS molecule to form a series chain, occupying the entire surface and forming micelle-like structures. Alternatively, the air-water interface may be fully occupied by CTAC alone as it is a much stronger surfactant, and PFBS is electrostatically paired with CTAC. Either way could lead to PFBS removal along with CTAC molecules from the water column during bubbling. Aerosol formation then removes enriched PFBS-CTAC from the solution (Fig. 4). Without a positively charged group (i.e., SDS and Brij® L4), the hydrophobic tail of the surfactant alone was not able to capture PFBS molecules.

3.4. Time-course experiments

We used 1 mg L⁻¹ CTAC and 0.01 M NaCl as our optimized condition and performed a series of time-course experiments for two short chains: PFBA and PFBS (Fig. 5). For PFBS ($C_0 = 0.5 \mu\text{g L}^{-1}$), 15 min of bubbling time was enough to remove PFBS to below detection (>99% removal, $<2 \text{ ng L}^{-1}$) (Fig. 5a). For PFBA, 120 min of bubbling time was not able to completely remove PFBA (66% removal), and the maximum removal was found at 60 min (81% removal) (Fig. 5a). We also measured the

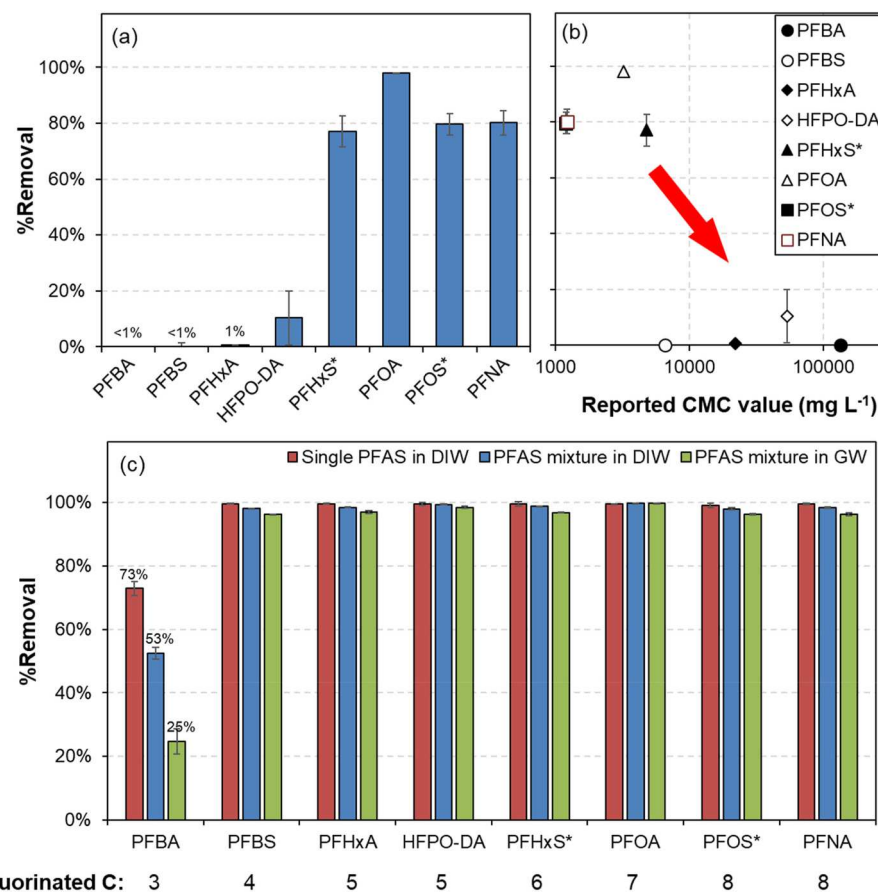


Fig. 6. Percentage removal of PFAS (%) under the optimized bubbling condition: (a) single PFAS prepared in deionized water without adding CTAC and (b) single PFAS removal percentage (no CTAC added) as a function of reported CMC values; (c) single and mixed PFAS prepared in deionized water/groundwater in the presence of CTAC. Asterisks represent total PFAS, the sum of branched and linear isomers. The initial concentration of each PFAS in the mixture was 2 nM. The error bar represents the standard deviation.

concentration of remaining CTAC in the solutions and the pattern over time was very similar to that of PFBA (Fig. 5b). The CTAC concentration decreased by $74 \pm 3\%$ in 30 min and stayed nearly constant till 120 min. Meanwhile, the thin foam layer at the surface disappeared gradually from 15 to 30 min. This echoes our finding in the previous section (Fig. 3b), where a threshold concentration of CTAC exists to lower the ST to generate a thin foam layer and initiate the removal process via aerosol formation. Continuously adding CTAC into the solution should be able to remove the remaining PFBA, as shown in a study in which a dosing pump was used to inject a co-foaming surfactant (CTAB, cetyltrimethylammonium bromide) continuously to maintain it at 2.1 mg CTAB L⁻¹ (Buckley et al., 2023a).

The increased PFBA concentration in the solution after 60 min (Fig. 5a) might be attributable to the condensed water (collected aerosols) on the lid that dripped down and brought PFBA back into the water. By calculating the PFAS mass from the bulk solution and condensed liquid on the lid collected, the mass balance of PFBS and PFBA in the time course experiments captured >70% of the total mass. The unbalanced mass was presumably enriched at the top surface layer ("thin" air-water interface), which we did not collect for the measurement.

3.5. Removal of single PFAS and PFAS mixtures using optimized conditions

We used our optimized condition (1 mg L⁻¹ CTAC and 0.01 M NaCl) to test other PFAS individually in MQW. Without the addition of CTAC, short-chain PFAS (e.g., PFBA, PFBS, PFHxA) and HFPO-DA (GenX) showed a very poor removal efficiency (0–10%) (Fig. 6a). The removal

percentage showed an inverse trend with the critical micelle concentration (CMC) of PFAS controlled by their chain length and functional group, and a lower CMC favors the propensity of foam fractionation and aerosolization by air bubbling (Fig. 6b). PFAS with a chain length higher than PFHxS (C6 PFSA) and PFOA (C8 PFCA) can be efficiently removed through foam fractionation in MQW without requiring CTAC addition. HFPO-DA is an alternative chemical for PFOA and its CMC (46000–60000 mg L⁻¹) is an order of magnitude higher than that of PFOA (~3200 mg L⁻¹), suggesting its lesser surface activity compared with long-chain PFCA. On the other hand, the CMC of HFPO-DA is slightly higher than PFHxA (C6 PFCA, CMC = ~22000 mg L⁻¹), but the percentage removal of HFPO-DA (~10%) was 10 times greater than PFHxA (~1%). This may be attributed to their structural differences, in which PFHxA possesses a six-carbon (C6) alkyl chain, and HFPO-DA is a perfluoroalkyl ether carboxylic acid (two C3 carbon chains separated by an oxygen atom).

With the addition of CTAC, most of the PFAS can be removed to below detection (>99% removal) except for PFBA (73% removal) (Fig. 6c). Next, we evaluated the efficiency of removing a mixture of eight PFAS fortified in two water types (MQW and groundwater matrix). Aside from PFBA, other compounds can achieve >99% removal (Fig. 6c). U.S. EPA recently announced the final National Primary Drinking Water Regulation (NPDWR) for six PFAS on April 10, 2024 (U.S. Environmental Protection Agency, 2024). Individual maximum contaminant levels (MCLs) were established for PFOA (4.0 ng L⁻¹), PFOS (4.0 ng L⁻¹), PFHxS (10 ng L⁻¹), PFNA (10 ng L⁻¹), and HFPO-DA (10 ng L⁻¹). The MCL for PFAS mixtures containing at least two or more of PFHxS, PFNA, HFPO-DA, and PFBS was calculated by a Hazard Index

<1 (HI, a sum of PFAS fractions where each fraction compares the level of each PFAS measured in the water to the health-based water concentration). Our results demonstrated that using CTAC-assisted bubbling/foam fractionation can rapidly remove the five regulated PFAS (PFOA, PFOS, PFHxS, PFNA, and HFPO-DA) from contaminated waters with ease to below their corresponding MCLs.

Notably, the removal percentage of PFBA declined (73% MW → 53% mixtures in MQW → 25% in groundwater) as the water matrix became complicated. This implies that coexisting ions (e.g., other PFAS) in the solution could compete with PFBA to interact with CTAC or displace PFBA from the electrostatic association with CTAC analogous to the early breakthrough occurring in GAC systems (Zhang et al., 2023). Additional bubbling time and sufficient cationic surfactants may be required to remove PFBA further while treating waters with a complex matrix (e.g., contaminated groundwater, wastewater, and landfill leachate). Buckley et al. (2023a) successfully removed nearly 100% PFBA in pure water within 60 min by air bubbling with a continuous feed of CTAB (2.1 mg L⁻¹), while the same device with similar conditions used in another study (Vo et al., 2023) failed to remove PFBA (~0%) in landfill leachate. Overall, the bubbling time and the dose of cationic surfactants as a function of complex water matrices to be treated require further investigation and optimization.

4. Conclusion

It is important to note that CTAC, belonging to the group of quaternary ammonium compounds (QACs), is also considered an emerging contaminant. Follow-up research should aim to identify greener and safer alternatives to CTAC for the efficient removal of short-chain PFAS via foam fractionation. For example, amino acid-based cationic surfactants might be an option because of their biodegradability, low toxicity, and green synthesis, which meets green chemistry requirements (Pérez et al., 2021). On the other hand, if CTAC is added to assist in removing PFAS in contaminated waters, an additional treatment step may be required (sorption or destruction methods) to remove residual CTAC in treated water. However, it could still be a worthwhile trade-off to applying QACs for PFAS elimination in waters because compared to PFAS (especially short-chain PFAS), QACs can be efficiently removed by GAC (Basar et al., 2004) and can also be rapidly destroyed by advanced oxidation processes (AOPs) like UV/H₂O₂ (Mondal et al., 2018). Moreover, QACs have been reported to increase the sorption capacity of GAC for PFOA via the bridging effect (Shaikh et al., 2023), which could be an added value to the overall treatment of PFAS.

Although the concept of foam fractionation is similar to DAF systems, our results highlight that a co-surfactant is required rather than a polyelectrolyte (e.g., PDM) to remove PFAS from non-foaming waters successfully. The foam formation and stability are critical for PFAS removal, as highlighted by the dose-dependent removal of PFAS in the presence of CTAC. Our results reveal that the ion pair formation between PFAS and the co-surfactant is the driving mechanism by which PFAS is removed in foam fractionation systems. The impact of co-occurring ions in the groundwater matrix was not investigated in the present study, but they were observed to impact the removal of short-chain PFAS. Hence, the sequential dosing of co-surfactant in a series of bubbling reactors may be needed to achieve treatment goals. Additionally, our mass balance study revealed that aerosolization was the primary pathway by which PFAS was removed from water. Aerosolization of PFAS was shown to be dominant in non-foaming waters in the present study and hence, the design of the reactor system will have to consider capturing aerosols to prevent atmospheric contamination. Future work should focus on the magnitude of PFAS aerosolization in varying matrices and as a function of bubble size and bubbling rates in the system.

CRediT authorship contribution statement

Cheng-Shiuan Lee: Writing – original draft, Methodology,

Investigation, Formal analysis, Conceptualization. **Arjun K. Venkatesan:** Writing – review & editing, Supervision, Methodology, Funding acquisition, Conceptualization.

Declaration of competing interest

The authors declare that they have no known competing financial interests or personal relationships that could have appeared to influence the work reported in this paper.

Data availability

Data will be made available on request.

Acknowledgment

The authors acknowledge the financial support of this work by the US Department of Defense's Strategic Environmental Research and Development Program (SERDP: ER22-3438) and the Division of Chemical, Bioengineering, Environmental and Transport Systems (CBET-2401203) of the US National Science Foundation. Thanks to the NYS Center for Clean Water Technology at Stony Brook University for their support during the course of the project. We also appreciate Dr. Carlos Colosqui in the Department of Mechanical Engineering at Stony Brook University for his support on surface tension measurements. The content is solely the responsibility of the authors and does not necessarily represent the official views of the sponsors.

Appendix A. Supplementary data

Supplementary data to this article can be found online at <https://doi.org/10.1016/j.chemosphere.2024.142614>.

References

Basar, C.A., Karagunduz, A., Cakici, A., Keskinler, B., 2004. Removal of surfactants by powdered activated carbon and microfiltration. *Water Res.* 38 (8), 2117–2124.

Bolto, B., Xie, Z., 2019. The use of polymers in the flotation treatment of wastewater. *Processes* 7 (6), 374.

Buck, R.C., Franklin, J., Berger, U., Conder, J.M., Cousins, I.T., de Voogt, P., Jensen, A.A., Kannan, K., Mabury, S.A., van Leeuwen, S.P., 2011. Perfluoroalkyl and polyfluoroalkyl substances in the environment: terminology, classification, and origins. *Integrated Environ. Assess. Manag.* 7 (4), 513–541.

Buckley, T., Karanam, K., Han, H., Vo, H.N.P., Shukla, P., Firouzi, M., Rudolph, V., 2023a. Effect of different co-foaming agents on PFAS removal from the environment by foam fractionation. *Water Res.* 230, 119532.

Buckley, T., Karanam, K., Xu, X., Shukla, P., Firouzi, M., Rudolph, V., 2022. Effect of mono- and di-valent cations on PFAS removal from water using foam fractionation—A modelling and experimental study. *Sep. Purif. Technol.* 286, 120508.

Buckley, T., Vuong, T., Karanam, K., Vo, P.H., Shukla, P., Firouzi, M., Rudolph, V., 2023b. Using foam fractionation to estimate PFAS air-water interface adsorption behaviour at ng/L and µg/L concentrations. *Water Res.* 239, 120028.

Burns, D.J., Hinrichsen, H.M., Stevenson, P., Murphy, P.J., 2022. Commercial-scale remediation of per- and polyfluoroalkyl substances from a landfill leachate catchment using Surface-Active Foam Fractionation (SAFF®). *Remediation* 32 (3), 139–150.

Burns, D.J., Stevenson, P., Murphy, P.J., 2021. PFAS removal from groundwaters using surface-active foam fractionation. *Remediation* 31 (4), 19–33.

Cao, Y., Lee, C., Davis, E.T., Si, W., Wang, F., Trimpin, S., Luo, L., 2019. 1000-Fold preconcentration of per- and polyfluorinated alkyl substances within 10 minutes via electrochemical aerosol formation. *Anal. Chem.* 91 (22), 14352–14358.

Costanza, J., Arshadi, M., Abriola, L.M., Pennell, K.D., 2019. Accumulation of PFOA and PFOS at the air–water interface. *Environ. Sci. Technol. Lett.* 6 (8), 487–491.

Dixit, F., Dutta, R., Barbeau, B., Berube, P., Mohseni, M., 2021. PFAS removal by ion exchange resins: a review. *Chemosphere* 272, 129777.

Du, Z., Deng, S., Bei, Y., Huang, Q., Wang, B., Huang, J., Yu, G., 2014. Adsorption behavior and mechanism of perfluorinated compounds on various adsorbents—a review. *J. Hazard Mater.* 274, 443–454.

Ebersbach, I., Ludwig, S.M., Constapel, M., Kling, H.-W., 2016. An alternative treatment method for fluorosurfactant-containing wastewater by aerosol-mediated separation. *Water Res.* 101, 333–340.

Evich, M.G., Davis, M.J., McCord, J.P., Acrey, B., Awkerman, J.A., Knappe, D.R., Lindstrom, A.B., Speth, T.F., Tebes-Stevens, C., Strynar, M.J., 2022. Per- and polyfluoroalkyl substances in the environment. *Science* 375 (6580), eabg9065.

Fenton, S.E., Ducatman, A., Boobis, A., DeWitt, J.C., Lau, C., Ng, C., Smith, J.S., Roberts, S.M., 2021. Per-and polyfluoroalkyl substance toxicity and human health review: current state of knowledge and strategies for informing future research. *Environ. Toxicol. Chem.* 40 (3), 606–630.

Franke, V., McCleaf, P., Lindegren, K., Ahrens, L., 2019. Efficient removal of per-and polyfluoroalkyl substances (PFASs) in drinking water treatment: nanofiltration combined with active carbon or anion exchange. *Environ. Sci.: Water Res. Technol.* 5 (11), 1836–1843.

Kucharzyk, K.H., Darlington, R., Benotti, M., Deeb, R., Hawley, E., 2017. Novel treatment technologies for PFAS compounds: a critical review. *J. Environ. Manag.* 204, 757–764.

Lee, Y.-C., Wang, P.-Y., Lo, S.-L., Huang, C., 2017. Recovery of perfluorooctane sulfonate (PFOS) and perfluorooctanoate (PFOA) from dilute water solution by foam flotation. *Sep. Purif. Technol.* 173, 280–285.

Li, Y.-F., Chien, W.-Y., Liu, Y.-J., Lee, Y.-C., Lo, S.-L., Hu, C.-Y., 2021. Perfluorooctanoic acid (PFOA) removal by flotation with cationic surfactants. *Chemosphere* 266, 128949.

Londhe, K., Lee, C.-S., Zhang, Y., Grdanovska, S., Kroc, T., Cooper, C.A., Venkatesan, A. K., 2021. Energy evaluation of electron beam treatment of perfluoroalkyl substances in water: a critical review. *ACS ES&T Engineering* 1 (5), 827–841.

Lu, D., Sha, S., Luo, J., Huang, Z., Jackie, X.Z., 2020. Treatment train approaches for the remediation of per-and polyfluoroalkyl substances (PFAS): a critical review. *J. Hazard Mater.* 386, 121963.

McCleaf, P., Kjellgren, Y., Ahrens, L., 2021. Foam fractionation removal of multiple per- and polyfluoroalkyl substances from landfill leachate. *AWWA Water Science* 3 (5), e1238.

Meng, P., Deng, S., Lu, X., Du, Z., Wang, B., Huang, J., Wang, Y., Yu, G., Xing, B., 2014. Role of air bubbles overlooked in the adsorption of perfluorooctanesulfonate on hydrophobic carbonaceous adsorbents. *Environ. Sci. Technol.* 48 (23), 13785–13792.

Meng, P., Deng, S., Maimaiti, A., Wang, B., Huang, J., Wang, Y., Cousins, I.T., Yu, G., 2018. Efficient removal of perfluorooctane sulfonate from aqueous film-forming foam solution by aeration-foam collection. *Chemosphere* 203, 263–270.

Meng, P., Jiang, X., Wang, B., Huang, J., Wang, Y., Yu, G., Cousins, I.T., Deng, S., 2020. Role of the air-water interface in removing perfluoroalkyl acids from drinking water by activated carbon treatment. *J. Hazard Mater.* 386, 121981.

Mondal, B., Adak, A., Datta, P., 2018. Effect of operating conditions and interfering substances on photochemical degradation of a cationic surfactant. *Environ. Technol.* 39 (21), 2771–2780.

Morrison, A.L., Strezov, V., Niven, R.K., Taylor, M.P., Wilson, S.P., Wang, J., Burns, D.J., Murphy, P.J., 2023. Impact of salinity and temperature on removal of PFAS species from water by aeration in the absence of additional surfactants: a novel application of green chemistry using adsorptive bubble fractionation. *Ind. Eng. Chem. Res.* 62 (13), 5635–5645.

Muensterman, D.J., Cahuas, L., Titaley, I.A., Schmokel, C., De la Cruz, F.B., Barlaz, M.A., Carignan, C.C., Peaslee, G.F., Field, J.A., 2022. Per-and polyfluoroalkyl substances (PFAS) in facemasks: potential source of human exposure to PFAS with implications for disposal to landfills. *Environ. Sci. Technol. Lett.* 9 (4), 320–326.

Nguyen, D., Stults, J., Devon, J., Novak, E., Lanza, H., Choi, Y., Lee, L., Schaefer, C.E., 2024. Removal of per-and polyfluoroalkyl substances from wastewater via aerosol capture. *J. Hazard Mater.* 465, 133460.

Nzeribe, B.N., Crimi, M., Mededovic Thagard, S., Holsen, T.M., 2019. Physico-chemical processes for the treatment of per-and polyfluoroalkyl substances (PFAS): a review. *Crit. Rev. Environ. Sci. Technol.* 49 (10), 866–915.

Pelch, K.E., Reade, A., Wolffe, T.A., Kwiatkowski, C.F., 2019. PFAS health effects database: protocol for a systematic evidence map. *Environ. Int.* 130, 104851.

Pérez, L., Pons, R., de Sousa, F.O., del Carmen Morán, M., da Silva, A.R., Pinazo, A., 2021. Green cationic arginine surfactants: influence of the polar head cationic character on the self-aggregation and biological properties. *J. Mol. Liq.* 339, 116819.

Rahman, M.F., Peldszus, S., Anderson, W.B., 2014. Behaviour and fate of perfluoroalkyl and polyfluoroalkyl substances (PFASs) in drinking water treatment: a review. *Water Res.* 50, 318–340.

Robey, N.M., da Silva, B.F., Annable, M.D., Townsend, T.G., Bowden, J.A., 2020. Concentrating per-and polyfluoroalkyl substances (PFAS) in municipal solid waste landfill leachate using foam separation. *Environ. Sci. Technol.* 54 (19), 12550–12559.

Schaefer, C.E., Culina, V., Nguyen, D., Field, J., 2019. Uptake of poly-and perfluoroalkyl substances at the air–water interface. *Environ. Sci. Technol.* 53 (21), 12442–12448.

Shaikh, M.A.N., Sarkar, P., Nawaz, T., 2023. PFOA remediation from aqueous media using CTAB impregnated activated carbon: a closed-loop sustainable study with comprehensive selectivity analysis. *J. Water Proc. Eng.* 54, 103965.

Smith, S.J., Lewis, J., Wiberg, K., Wall, E., Ahrens, L., 2023. Foam fractionation for removal of per-and polyfluoroalkyl substances: towards closing the mass balance. *Sci. Total Environ.* 871, 162050.

Smith, S.J., Wiberg, K., McCleaf, P., Ahrens, L., 2022. Pilot-scale continuous foam fractionation for the removal of per-and polyfluoroalkyl substances (PFAS) from landfill leachate. *ACS Es&t Water* 2 (5), 841–851.

Sunderland, E.M., Hu, X.C., Dassuncao, C., Tokranov, A.K., Wagner, C.C., Allen, J.G., 2019. A review of the pathways of human exposure to poly-and perfluoroalkyl substances (PFASs) and present understanding of health effects. *J. Expo. Sci. Environ. Epidemiol.* 29 (2), 131–147.

Thompson, J., Eaglesham, G., Reungoat, J., Poussade, Y., Bartkow, M., Lawrence, M., Mueller, J.F., 2011. Removal of PFOS, PFOA and other perfluoroalkyl acids at water reclamation plants in South East Queensland Australia. *Chemosphere* 82 (1), 9–17.

Thompson, J.T., Chen, B., Bowden, J.A., Townsend, T.G., 2023. Per-and polyfluoroalkyl substances in toilet paper and the impact on wastewater systems. *Environ. Sci. Technol. Lett.* 10 (3), 234–239.

U.S. Environmental Protection Agency, 2023. CompTox Chemicals Dashboard. <https://comptox.epa.gov/dashboard/>.

U.S. Environmental Protection Agency. Per- and Polyfluoroalkyl Substances (PFAS): Final PFAS National Primary Drinking Water Regulation. <https://www.epa.gov/sdwa/and-polyfluoroalkyl-substances-pfas#Summary>.

Venkatesan, A.K., Halden, R.U., 2013. National inventory of perfluoroalkyl substances in archived US biosolids from the 2001 EPA National Sewage Sludge Survey. *J. Hazard Mater.* 252, 413–418.

Venkatesan, A.K., Lee, C.-S., Gobler, C.J., 2022. Hydroxyl-radical based advanced oxidation processes can increase perfluoroalkyl substances beyond drinking water standards: results from a pilot study. *Sci. Total Environ.* 847, 157577.

Vo, P.H., Buckley, T., Xu, X., Nguyen, T.M.H., Rudolph, V., Shukla, P., 2023. Foam fractionation of per-and polyfluoroalkyl substances (PFASs) in landfill leachate using different cosurfactants. *Chemosphere* 310, 136869.

Wang, W., Du, Z., Deng, S., Vakili, M., Ren, L., Meng, P., Maimaiti, A., Wang, B., Huang, J., Wang, Y., 2018. Regeneration of PFOS loaded activated carbon by hot water and subsequent aeration enrichment of PFOS from eluent. *Carbon* 134, 199–206.

Wang, Y., Ji, Y., Tishchenko, V., Huang, Q., 2023. Removing per-and polyfluoroalkyl substances (PFAS) in water by foam fractionation. *Chemosphere* 311, 137004.

Xia, C., Diamond, M.L., Peaslee, G.F., Peng, H., Blum, A., Wang, Z., Shalin, A., Whitehead, H.D., Green, M., Schwartz-Narbonne, H., 2022. Per-and polyfluoroalkyl substances in North American school uniforms. *Environ. Sci. Technol.* 56 (19), 13845–13857.

Yefet, S., Sloutskin, E., Tamam, L., Sapir, Z., Deutsch, M., Ocko, B.M., 2014. Surfactant-induced phases in water-supported alkane monolayers: II. Structure. *Langmuir* 30 (27), 8010–8019.

Zhang, W., Liang, Y., 2020. Removal of eight perfluoroalkyl acids from aqueous solutions by aeration and duckweed. *Sci. Total Environ.*, 138357.

Zhang, Y., Thomas, A., Apul, O., Venkatesan, A.K., 2023. Coexisting ions and long-chain per-and polyfluoroalkyl substances (PFAS) inhibit the adsorption of short-chain PFAS by granular activated carbon. *J. Hazard Mater.* 460, 132378.